

Wear behaviours of Al_2O_3 ceramic tool when machining typical workpiece materials based on thermodynamic characteristics

Cutting temperature always highly reaches over to 1000°C during high speed machining with Al_2O_3 ceramic tools. Diffusion wear is the main wear mechanisms at such high temperature. In this paper, the rules of diffusion wear for Al_2O_3 ceramic tools are studied based on thermodynamics. Dissolution concentrations in typical normal workpiece materials of ceramic tool material at different temperatures are then calculated. Diffusion reaction rules in high temperature are also analyzed using Gibbs free energy criterion, it is found that the theoretical results are uniform with the experimental data; and the diffusion solubility of Al_2O_3 ceramic tools is usually much smaller. The order of dissolution of Al_2O_3 ceramic tools in machining several typical normal workpieces is as follows: titanium > nickel > steel. At the same cutting condition, when machining cast iron and 35# steel, the wear performance of tools is very different and the wear mechanism should be researched more. The results will provide useful references for tool material design and selection.

Keywords: Thermodynamics characteristics, Al_2O_3 ceramic tool, wear behaviour

1. Introduction

Tool wear is always a main problem in cutting region because the diffusion wear of tool not only influences the machining precision and surface quality, but also possibly leads to cutting flutter as well as the damage of machine, tool and workpiece and so on^[1]. Therefore the measures such as the research on the mechanism of tool wear, the prediction and supervision to tool wear and the exchange of new knife or blade in good time before the sharp wear for tool are more important, which not only can

guarantee the work reliability for the machining system and enhance the product quality, but also can give full play to the cutting performance for tool, increase production efficiency and economic benefit. In this way, the research on the wear rules has the important actual significance.

As with the excellent synthetical performance such as high strength, high rigidity, anti-corrosion, anti-thermal shock, anti-creep and stable structure and so on, ceramic has become a much more appropriate engineering ceramic material^[2], the allowable cutting temperature can highly reach over to 1000°C and the cutting speed can also reach over to 100m/min when cutting medium carbon steel. With the increase of cutting speed and cutting temperature, the wear mechanism of tool becomes more complex. Oliver Hatt et al^[3]. considered that the mechanism of tool wear and damage were essentially different from that of the common cutting; during high speed cutting; the tool would be with different failure mechanisms under the much worse work condition than that for the common cutting process, and the influence of cutting temperature and thermal stress to the wear and damage for tool would become more prominent. Elyas et al^[4] researched the friction for Al_2O_3 ceramic tool respectively in dry friction and work lubrication conditions and made a conclusion that the dissolution wear and diffusion wear were ubiquitous in high temperature; the diffusion wear for ceramic tool changed the performance for tool material and also influenced its reliability. Murthy, T.S.R.C et al^[5] researched the wear conformation and mechanism when matching of every kind of tool material with workpiece material during high speed cutting.

The tool wear is a process affected by many nonlinear and high coupling factors. Thermodynamics supplies a systemic analysis method to nonlinear mutual effect among many factors. Therefore it is very reasonable and feasible to reach the wear process by using of thermodynamics theory and method^[6]. However, the research on the mechanism of tool wear from thermodynamics view is still few.

In this paper, the research on diffusion wear and oxidation wear for ceramic tools during high speed cutting by using thermodynamics theory is advanced, which is to analyze the

Messrs. Fang Shao*, Jiang Hongwan and Aijun Liu, School of Mechanical Engineering, Guizhou Institute of Technology, Guiyang 550003, China; Renwei Wang, School of Mechanical Engineering, Shandong University, Jinan 250061, China; Chengcheng Niu, Key Laboratory of Advanced Manufacturing Technology, Ministry of Education, Guizhou University, Guiyang 550025, China; Fa Zhang, School of Mechanical Engineering, Guizhou University, Guiyang 550025, China; Xiao Lihua, Center of Analysis and Testing, Guizhou Institute of Technology, Guiyang, 550003, China; Kesheng Zhang, School of Electrical and Information Engineering, Guizhou Institute of Technology, Guiyang 550003, China

*Corresponding author

diffusion and oxidation wear rules for ceramic tools by the calculation of thermodynamics parameters in the cutting process, and moreover to direct the application of ceramic tools and supply reference for the design and optimization for tool materials according to the research conclusion.

2. Diffusion wear for Al₂O₃ ceramic tools

In 1855, Fick^[7] concluded a diffusion relation quantitatively in isotropy medium by means of heat conduction method based on the corresponding experiments, i.e. Diffusion First-Law:

$$J = D \frac{\partial C}{\partial \varphi}$$

Where: J is diffusion flux, i.e. diffusion gross amount passing unit section vertical to diffusion direction in unit time; C is volume concentration, i.e. atom amount of diffusion material in unit volume; $\partial C/\partial \varphi$ – concentration gradient; D is diffusion coefficient, $D=D_0 \exp[-Q/RT]$, Where, D₀ is diffusion constant (m²/s), Q is diffused activation energy (J/mol), R is gas constant, which equals to 8.314, [J/(mol.K)], T is thermodynamic temperature (K).

In the cutting process, because of high temperature in cutting region as well as the compact contact between fore-and-aft blades of tools and the new-cutting surface, there are much greater chemical activity among cutting scraps, workpiece and fore-and-aft blades. In this way, the chemical elements in the contact surface between tool materials and workpiece materials may be diffused to each other, so as to change their chemical components and influence cutting performance. During high speed cutting, workpiece materials continuously flow in cutting distortion region, and moreover diffusion flux J is also kept in high degree among diffusion sections. Strong plastic deformation of workpiece materials will also increase dislocation density and interstice. All of these factors lead to intensify this mutual diffusion greatly.

According to Second-Law of Thermodynamics, the change of Gibbs free energy is a criterion to judge whether one reaction or change can take place spontaneously or not in constant temperature and pressure. This criterion not only can judge the direction for one chemical reaction, but also can be used for judging diffusion rules when workpiece is processed by tools^[8]. Suppose A is tool material, B is workpiece material, judge whether elements in A diffused in elements in B can be concluded by calculating Gibbs free energy after diffusion:

$$\Delta G_m = \Delta H_m - T\Delta S_m \quad (1)$$

$$\Delta H_m = H_{AB} - H_A - H_B \quad (2)$$

$$T\Delta S_m = RT(x_A \ln x_A + \ln x_B) \quad (3)$$

Where: ΔG_m is Gibbs free energy for diffusion reaction; ΔH_m is enthalpy after diffusion mixing; ΔS_m is mixing enthalpy after diffusion; H_i is enthalpy for each component; x_i is concentration for each component ($x_A + x_B = 1$);

If $\Delta G_m > 0$, diffusion does not happen, $\Delta G_m = 0$ reaction reaches to balance; only if $\Delta G_m < 0$, diffusion happens, therefore the optimal combination for blade-workpiece materials is as follows according to Equation (1), (2) and (3).

ΔH_m is a positive with much greater absolute value, i.e. $H_{AB} = 0$, and H_A, H_B are all negative with much greater absolute value. Only in this way, ΔG_m will be greater than zero, therefore this means that the diffusion does not happen or hardly happen in these two materials. Next, we will analyze the diffusion wear rules for Al₂O₃ ceramic tool from two aspects including enthalpy value and diffusion concentration.

2.1 STANDARD HEAT OF FORMATION $\Delta_f H^\ominus$ FOR COMPOUND AND ENTHALPY VALUE ANALYSIS IN DIFFERENT TEMPERATURE

In temperature T and standard pressure P[⊙], reaction heat for 1mol compound formatted by elementary substance in the most stable state is called standard mol enthalpy of formation or standard formation heat for this compound^[8]. The traditional ceramic tools include alumina ceramic tools and silicon nitride ceramic tools; the standard formation heats for alumina ceramic and silicon nitride respectively are as follows.

Standard formation heat $\Delta_f H^\ominus$ for Al₂O₃ :

$$\Delta_f H^\ominus = -1675274 \text{ J} \cdot \text{mol}^{-1}$$

Standard formation heat $\Delta_f H^\ominus$ for Si₃N₄:

$$\Delta_f H^\ominus = -744752 \text{ J} \cdot \text{mol}^{-1}$$

The absolute enthalpies $H^\ominus = (H_T^\ominus - H_{298}^\ominus) + H_{298}^\ominus$ are calculated at different temperature according to the relative enthalpies $(H_T^\ominus - H_{298}^\ominus)$ for Al₂O₃ and Si₃N₄ obtained by thermodynamics data table^[9], which can be seen in Table 1 and Fig. 1.

Analysis and discussion

1. From Fig. 1, enthalpies of Al₂O₃ and Si₃N₄ are all increased with the increase of temperature, therefore diffusion degree between tools material and workpiece material also will strengthen with the increase of temperature.
2. From Equation (1) $\Delta H_m = H_{AB} - H_A - H_B$, suppose that solid solution is ideal solution formed by the dissolution in workpiece material after the decomposition of Al₂O₃ and Si₃N₄, i.e. the formed solid solution accords with Raoult's Law^[3], therefore mixing enthalpies H_{AB} between Al₂O₃ and workpiece as well as Si₃N₄ and workpiece respectively equal to zero; in addition, because the

absolute enthalpies of Al_2O_3 is greatest, therefore the mixing enthalpies ΔH_m of Al_2O_3 is greatest. From this view, at the same temperature, diffusion reaction will hardly happen; besides, it also indicates that Al_2O_3 is much more propitious to be used as tools material than Si_3N_4 in diffusion aspect because the activity of Al_2O_3 is larger than that of Si_3N_4 . Next, we take Al_2O_3 ceramic tools as example to analyze diffusion wear rules.

TABLE 1. ABSOLUTE ENTHALPIES AND RELATIVE ENTHALPIES AT DIFFERENT TEMPERATURE OF Al_2O_3 AND Si_3N_4 ($\text{J}\cdot\text{MOL}^{-1}$)

Temperature / K	Al_2O_3		Si_3N_4	
	$H_T^\ominus - H_{298}^\ominus$	H_T^\ominus	$H_T^\ominus - H_{298}^\ominus$	H_T^\ominus
298	0	-1675274	0	-744752
300	158	-1675116	198	-744554
400	9039	-1666235	10768	-733984
500	19151	-1656123	22430	-722322
600	30011	-1645263	35020	-709732
700	41411	-1633863	48437	-696315
800	53247	-1622027	62605	-682147
900	65408	-1609866	77456	-667296
1000	77795	-1597479	92928	-651824
1100	90372	-1584902	108962	-635790
1200	103115	-1572159	125501	-619251
1300	116005	-1559269	142488	-602264
1400	129032	-1546242	159868	-584884
1500	142186	-1533088	177585	-567167

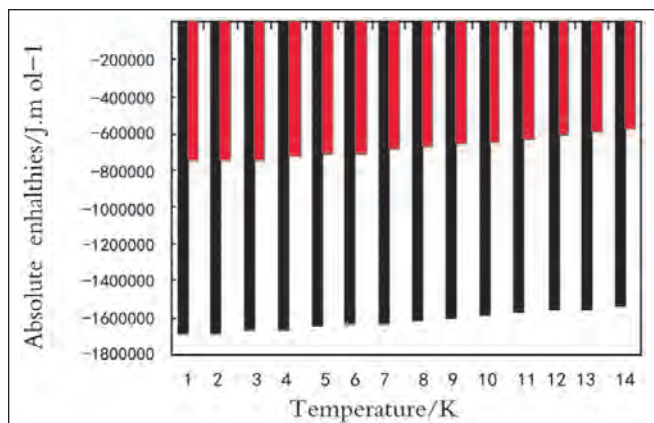


Fig. 1: Absolute enthalpies at different temperatures of Al_2O_3 (back) and Si_3N_4 (red)

2.2 ANALYSIS THE CHANGE OF GIBBS FREE ENERGY AND CONCENTRATION FOR Al_2O_3 AND Si_3N_4 RESPECTIVELY MELTED INTO EACH WORKPIECE MATERIAL

Gibbs free energy is also called free energy, whose calculation equation is as follows:

$$G = U + pV - TS$$

Where, U, p, V, T, S are respectively internal energy, pressure,

volume, temperature and entropy; the change of Gibbs free energy is a criterion to judge whether one reaction or change can take place spontaneously or not in constant temperature and pressure, and if $\Delta G < 0$ diffusion happens spontaneously, $\Delta G = 0$ reaction reaches to balance and $\Delta G > 0$, diffusion does not happen^[8]. Next, we will analyze the diffusion rules for carbide-tipped tool from the change of Gibbs free energy. In much higher speed cutting, wear mechanism for tools is a dissolving diffusion wear; suppose that tools material is AxByCz , therefore the formed free energy for tools material can be calculated as the following equation^[10]:

$$\Delta G_{f,\text{AxByCz}}^\ominus = x\Delta\bar{G}_A + y\Delta\bar{G}_B + z\Delta\bar{G}_C \quad (4)$$

Where $\Delta G_{f,\text{AxByCz}}^\ominus$ is the formed free energy when tools material AxByCz dissolves and diffused in tool-workpiece solution; $\Delta\bar{G}_i$ ($i = A, B$ or C) is relative mol free energy of element I for tools material in solid solution.

According to thermodynamics theory, the following equation can be obtained:

$$\Delta\bar{G}_i = \Delta(\Delta\bar{G}_i^{\text{xs}}) + RT\ln c_i \quad (5)$$

Where: $\Delta\bar{G}_i^{\text{xs}}$ is excess free energy of solid solution formed by each element A, B, C in tools material; R is mol gas constant; c_i is solubility expressed by mole fraction for element i of tool material in workpiece material.

Combine with (4) and (5), and then:

$$\Delta G_{f,\text{AxByCz}}^\ominus = x\Delta\bar{G}_A + y\Delta\bar{G}_B + z\Delta\bar{G}_C = \Delta\bar{G}_i^{\text{xs}} + RT(x\ln c_A + y\ln c_B + z\ln c_C)$$

where, $\Delta\bar{G}_i^{\text{xs}} = x\Delta\bar{G}_A + y\Delta\bar{G}_B + z\Delta\bar{G}_C$

and then solubility of tool material in workpiece material is as follows:

$$C_{\text{AxByCz}} = \exp\left(\frac{\Delta G_{f,\text{AxByCz}}^\ominus - \Delta G^{\text{xs}} - RTM}{NRT}\right) \quad (6)$$

Where, C_{AxByCz} is solubility of tool material in workpiece material; $M = x\ln x + y\ln y + z\ln z$; $N = X + Y + Z$.

Therefore, if we know the formed free energy $\Delta G_{f,\text{AxByCz}}^\ominus$ of tools material at different temperature and excess free energy $\Delta\bar{G}_i^{\text{xs}}$ of solid solution formed by each element in tools material, and then limit solubility of tools material in workpiece material can be calculated according to Equation (6), which can also make the prediction to tools wear state.

(1) Diffusion solubility of Al_2O_3 ceramic tools with Fe element when machining steel material.

Excess free energy of aluminum in $\text{Fe}^{[11]}$ is $\Delta\bar{G}_1^{\text{xs}} = -44.8$ ($\text{kJ}\cdot\text{mol}^{-1}$) and that of oxygen in $\text{Fe}^{[11]}$ is $\Delta\bar{G}_2^{\text{xs}} = 52.7$ ($\text{kJ}\cdot\text{mol}^{-1}$), therefore, solubility of tools material for Al_2O_3 ceramic tools when machining steel material can be calculated as the following equation:

$$C_{\text{Al}_2\text{O}_3} = \exp\left(\frac{\Delta G_{\text{Al}_2\text{O}_3} - 38.91T - 68500}{41.57T}\right) \quad (7)$$

(2) Diffusion solubility of Al_2O_3 ceramic tools with titanium element when machining titanium alloy

Solubility of aluminum in β titanium at $1470^\circ C$ is 33%^[12], and then solubility of Al_2O_3 in β titanium is half of 33%, i.e. 16.5%; therefore, excess free energy of oxygen in titanium can be obtained by adverse-calculation method. From literature^[3], the relationship between standard formation Gibbs free energy of Al_2O_3 and temperature can expressed as follows: $\Delta G = -1682900 + 323.24T$; the temperature range is from $660^\circ C$ to $2042^\circ C$, therefore, standard formed Gibbs free energy of Al_2O_3 at $1470^\circ C$ (i.e. 1743K) equals to $-1119492J$. According to Equation (6), the following equation can be obtained:

$$0.165 = \exp\left(\frac{-1119492.68 - (\Delta G_{O \text{ in titanium}}^{xs} + \Delta G_{Al \text{ in titanium}}^{xs}) - 8.314 \cdot 1743(2\ln 2 + 3\ln 3)}{5 \cdot 8.314 \cdot 1743}\right)$$

Therefore

$$\Delta G_{O \text{ in titanium}}^{xs} + \Delta G_{Al \text{ in titanium}}^{xs} = -1056789.8$$

Therefore, solubility of Al_2O_3 ceramic tools in titanium alloy material can be obtained as follows:

$$C_{Al_2O_3} = \exp\left(\frac{\Delta G_{Al_2O_3} - 38.91T - 1056789.8}{41.57T}\right) \quad (8)$$

(3) Diffusion solubility of Al_2O_3 ceramic tools when machining aluminum alloy

Excess free energy of aluminum in aluminum is zero and solubility of oxygen in aluminum is hardly zero; Al_2O_3 is a compound with much stronger chemical stability, which is hard to be composed and decomposed, therefore the possibility for diffusion wear is very small. However, tools and workpiece material are all with aluminum element, which leads to much better compatibility for each other; therefore workpiece material is easy to cling on tool surface.

(4) Diffusion solubility of Al_2O_3 ceramic tools when machining nickel

Solubility of oxygen in nickel at $1440^\circ C$ is 0.6%^[4]; because the solubility of aluminum in nickel at $1360^\circ C$ (i.e. 1633K) is 11%, and then the solubility of Al_2O_3 in nickel is half of 11%, i.e. 5.5%; therefore, according to Equation $\Delta G = -1682900 + 323.24T$, standard formed Gibbs free energy of Al_2O_3 at $1360^\circ C$ (i.e. 1633K) equals to -1155049.08 . According to Equation (6), the following equation can be obtained:

$$0.005 = \exp\left(\frac{-1155049.08 - (\Delta G_{O \text{ in nickel}}^{xs} + \Delta G_{Al \text{ in nickel}}^{xs}) - 8.314 \cdot 1633(2\ln 2 + 3\ln 3)}{5 \cdot 8.314 \cdot 1633}\right)$$

TABLE 2. SOLUBILITY OF Al_2O_3 CERAMIC TOOL WHEN MACHINING TYPICAL MATERIALS AT DIFFERENT TEMPERATURE

Solubility	933	1000	1200	1400	1500	1600	1613	1700	1743	1800
Fe	2.28618E-17	4.71E-16	5.28E-13	7.96E-11	5.92E-10	3.42E-09	4.23E-09	1.61E-08	2.97E-08	6.39E-08
Ni	3.68982E-05	0.000116	0.001638	0.010879	0.023202	0.045012	0.048767	0.080776	0.101746	0.135836
Ti	9.11146E-05	0.000269	0.003308	0.019871	0.04071	0.076253	0.082263	0.13266	0.165067	0.217021

Therefore

$$\Delta G_{O \text{ in nickel}}^{xs} + \Delta G_{Al \text{ in nickel}}^{xs} = -1021730.07$$

Therefore, solubility of Al_2O_3 ceramic tools in nickel material can be obtained as follows:

$$C_{Al_2O_3} = \exp\left(\frac{\Delta G_{Al_2O_3} - 38.91T - 1021730.07}{41.57T}\right) \quad (8)$$

Solubility of Al_2O_3 ceramic tools when respectively machining steel material, titanium alloy, aluminum alloy and pure nickel is depicted in Table 2 and Fig. 2.

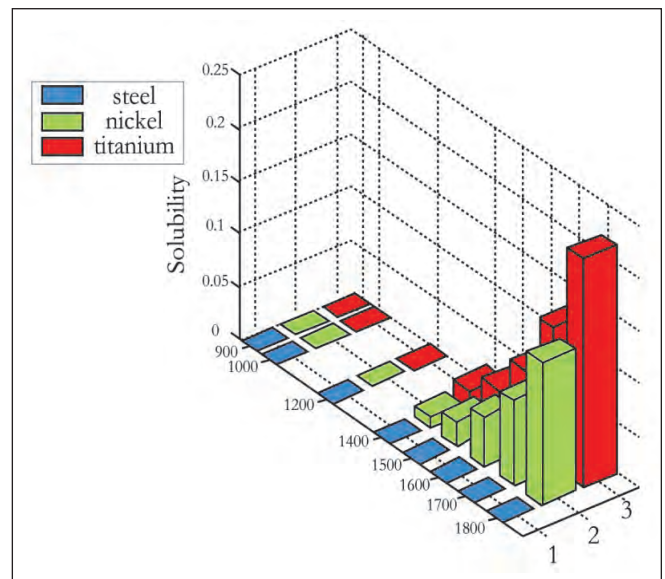


Fig.2: Solubility of Al_2O_3 ceramic in typical workpiece materials

3. Experiments

3.1 EXPERIMENT DEVICE

PUMA300LM numerically-controlled machine tool

3.2 EXPERIMENT MATERIALS

Aluminum alloy material, rigidity 115HBW, diameter $\phi 54.5mm$; stainless steel material, rigidity 184HBW, diameter $\phi 47mm$; abrasion resistant cast iron MT-4 cast iron material (cast iron for short hereinafter), rigidity 184HBW, diameter $\phi 42mm$; 35# steel material, rigidity 169HBW, diameter $\phi 48mm$; pure nickel material, rigidity 51.9HBW, diameter $\phi 28mm$; titanium alloy material, rigidity 41.9HBW, diameter $\phi 21mm$. The components of workpiece material are depicted in Tables 3 to 6.

TABLE 3. CHEMICAL COMPONENTS OF CAST IRON(%)

Element	C	Si	S	P	Cr Ni Cu Al Mo V	Fe
Content	3.38	2.1	0.121	0.072	Little	Other

TABLE 4. CHEMICAL COMPONENTS OF STAINLESS STEEL (%)

Element	Cr	Ni	C	Si	Mn	P
Content	16.63	4.7	0.072	0.488	7.692	0.027

TABLE 5. CHEMICAL COMPONENTS OF 35 STEEL (%)

Element	C	Si	Mn	S	P	Cr
Content	0.384	0.213	0.564	0.035	0.036	0.25

TABLE 6. CHEMICAL COMPONENTS OF ALUMINUM ALLOY (%)

Element	Si	Cu	Mg	Ni	Mn	Ti
Content	11.5-13.0	0.8-1.3	0.8-1.3	0.8-1.3	≤0.15	≤0.2

Nickel is pure nickel; component of titanium alloy is 73.68% of titanium and 26.32% of aluminum.

3.3 TOOLS

ISCAR tools produced bin Israel

3.4 CUTTING CONDITION AND MEASUREMENT RESULTS CAN BE SEEN IN TABLE 7.

TABLE 7. CUTTING CONDITION AND MEASUREMENT RESULTS

Workpiece material	a_p (mm)	f (mm/r)	V (m/min)	Cutting temperature (°C) (with low precision, only for comparison and reference)
Cast iron	5	0.3	150	92
Nickel	1	0.2	100	82
Stainless steel	2.5	0.2	150	36
Titanium alloy	2	0.2	150	75
Aluminum alloy	1	0.2	250	34
35# steel	1	0.2	150	38

3.5 EXPERIMENT PROCESS

Cutting six workpiece materials on PUMA300LM numerically-controlled machine tool; in order to analyze diffusion and oxidation wear character, select points to make energy spectrum analysis in the bottom of wear region or non-cutting region. In addition, in order to decrease the influence of pollution factors in tool surface, make line scanning on blade surface, the line scanning results for element aluminum, oxygen and titanium of tools material when machining nickel, aluminum alloy, 35# steel and cast iron can be seen in Figs. 3 to 25.

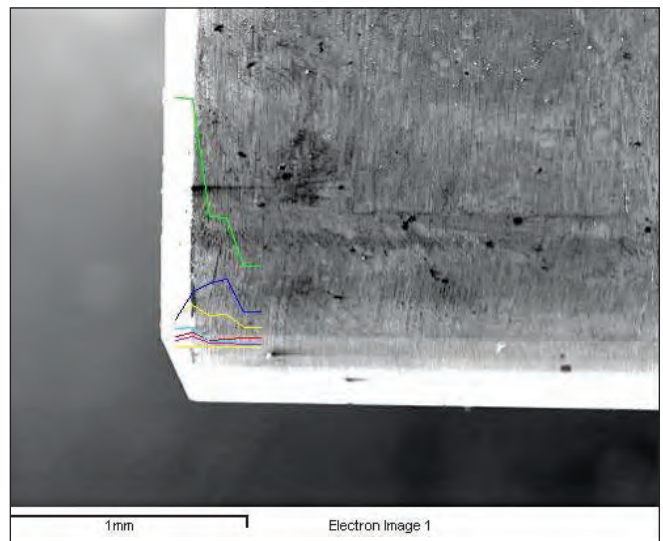


Fig. 3: Line scanning when machining nickel

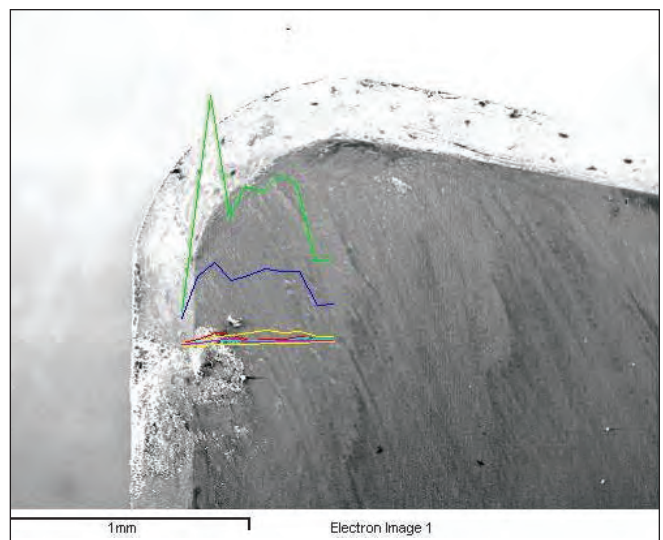


Fig. 4: Line scanning when machining titanium nickel

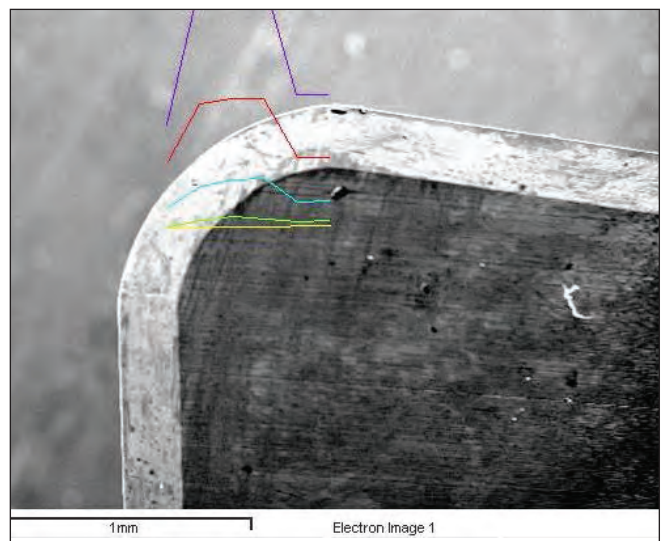


Fig. 5: Line scanning when machining 35# steel

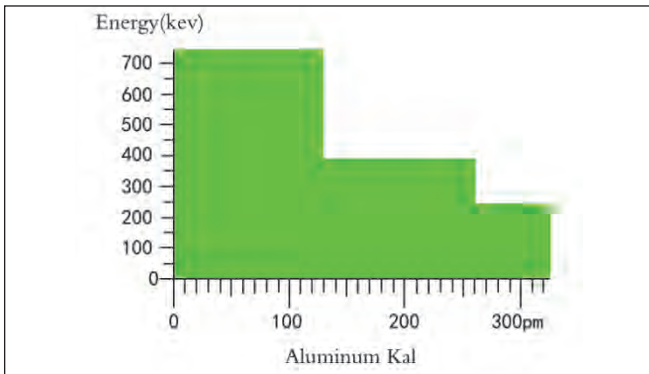


Fig. 6: Elements components of aluminum in line scanning when machining nickel

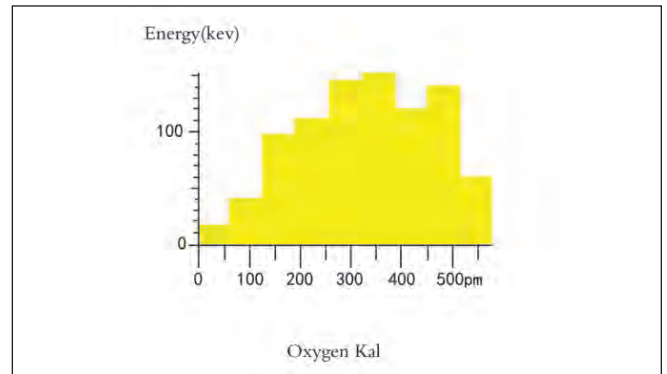


Fig. 10: Elements components of oxygen in line scanning when machining titanium based alloy

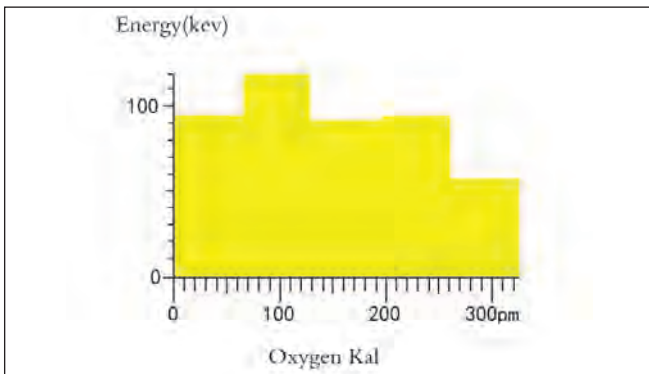


Fig. 7: Elements components of oxygen in line scanning when machining nickel

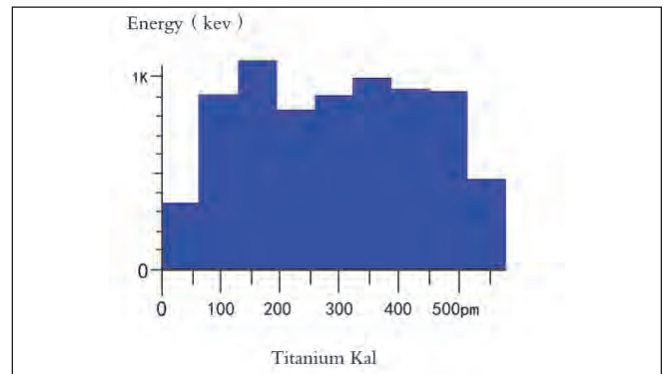


Fig. 11: Elements components of titanium in line scanning when machining titanium based alloy

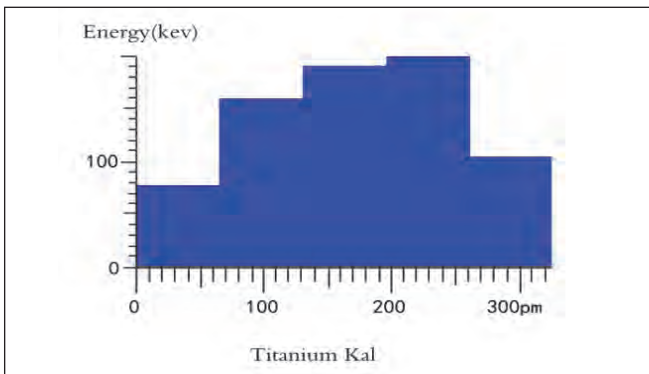


Fig. 8: Elements components of titanium in line scanning when machining nickel

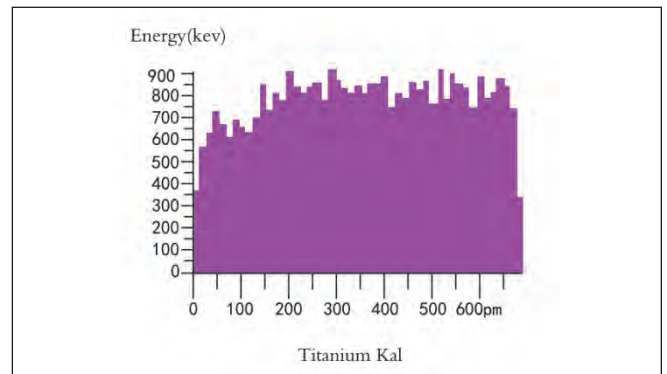


Fig. 12: Elements components of aluminum in line scanning when machining 35# steel

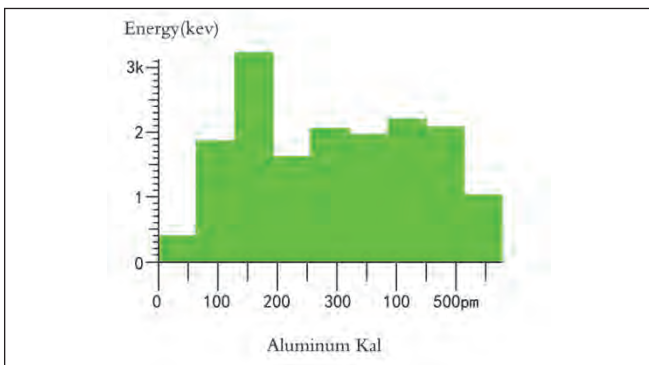


Fig. 9: Elements components of aluminum in line scanning when machining titanium based alloy

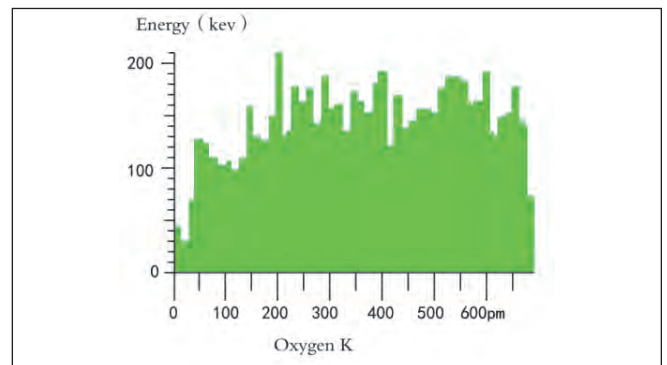


Fig. 13: Elements components of oxygen in line scanning when machining 35# steel

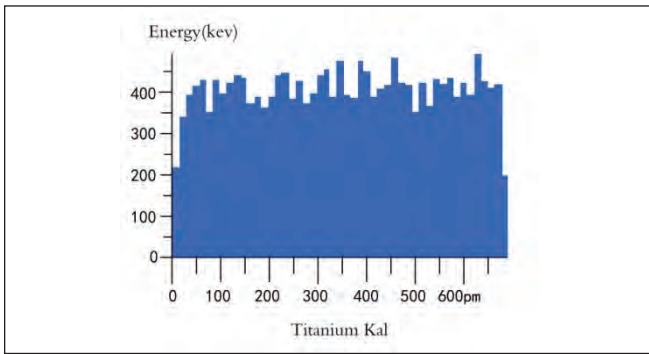


Fig. 14: Elements components of titanium in line scanning when machining 35# steel

Element	Weight%	Atomic%
O K	0.81	2.86
Al K	1.77	3.70
Ni K	97.42	93.44
Totals	100.00	

Fig. 15: Elements of chip when machining nickel

Element	Weight%	Atomic%
C K	20.22	35.46
O K	20.42	26.89
Al K	33.62	26.25
Si K	0.39	0.30
Ti K	24.60	10.82
Totals	100.00	

Fig. 16: Elements of chip when machining titanium-aluminum alloy

Element	Weight%	Atomic%
O K	7.83	22.87
Mn K	0.57	0.49
FeK	91.60	76.64
Totals	100.00	

Fig. 17: Elements of chip when machining 35# steel

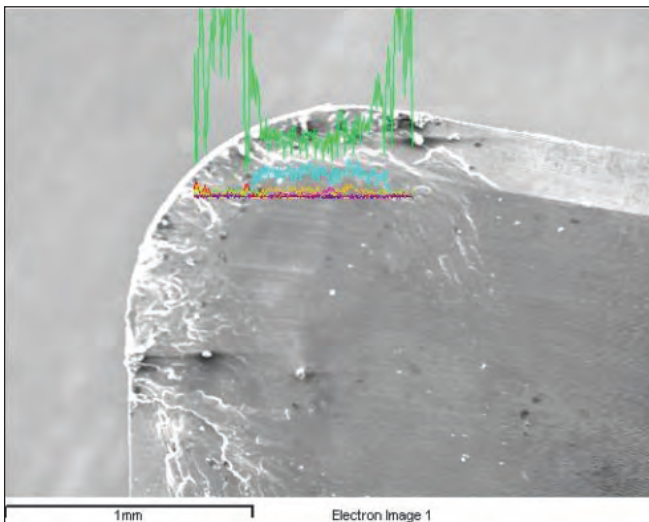


Fig. 18: Line scanning when machining aluminum alloy

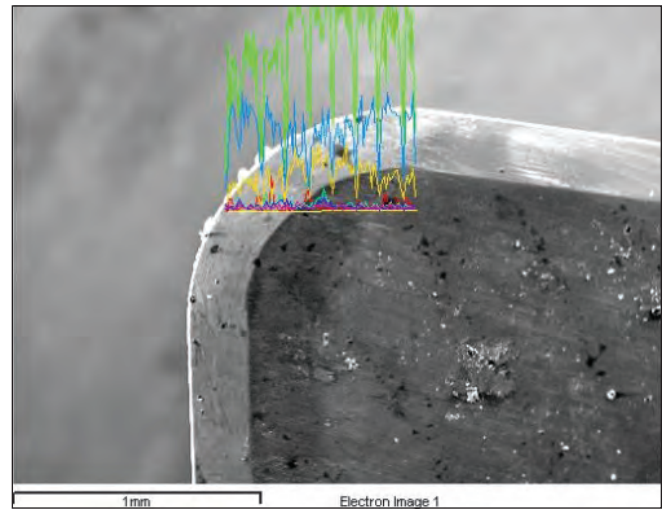


Fig. 19: Line scanning when machining cast iron

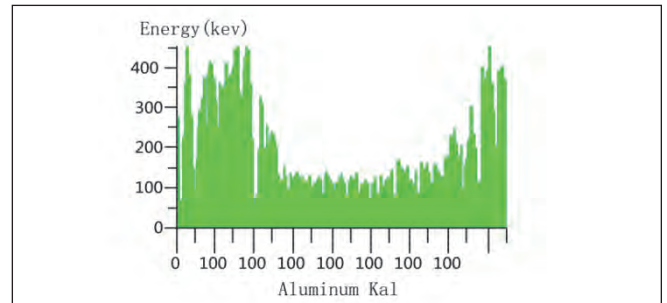


Fig. 20: Elements components of aluminum in line scanning when machining aluminum alloy

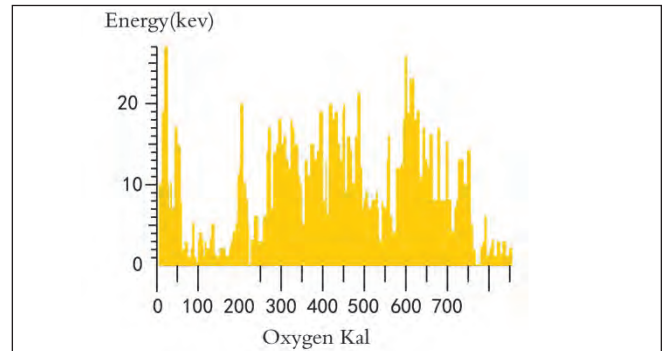


Fig. 21: Elements components of oxygen in line scanning when machining aluminum alloy

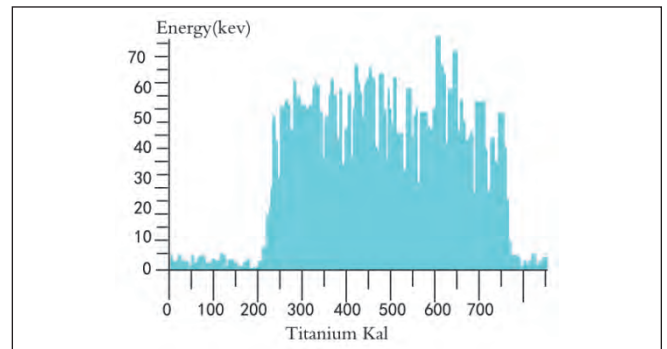


Fig. 22: Elements components of titanium in line scanning when machining aluminum alloy

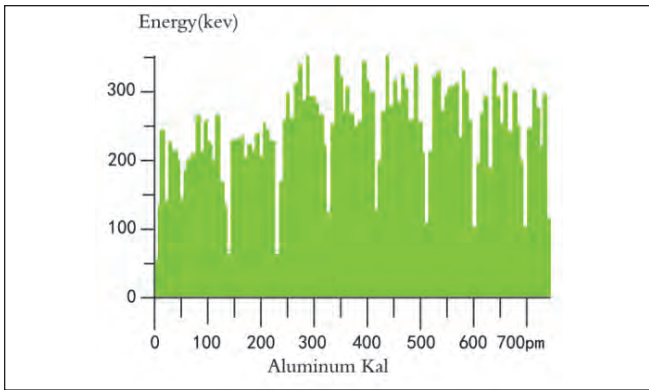


Fig. 23: Elements components of aluminum in line scanning when machining cast iron

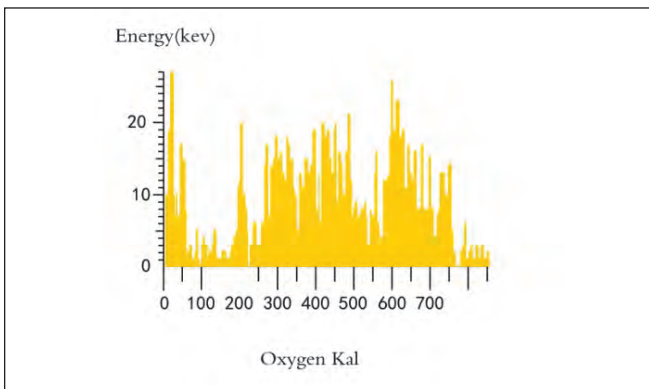


Fig. 24: Elements components of oxygen in line scanning when machining cast iron

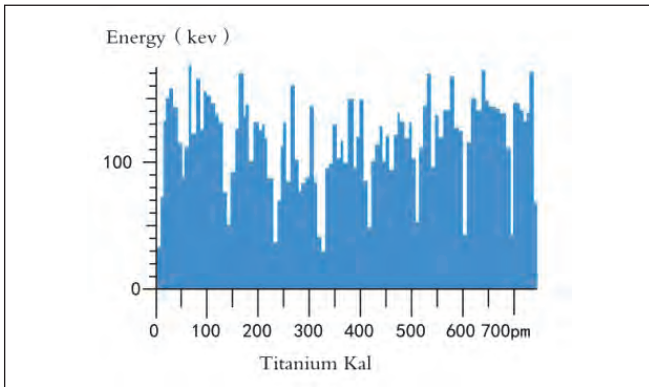


Fig. 25: Elements components of titanium in line scanning when machining cast iron

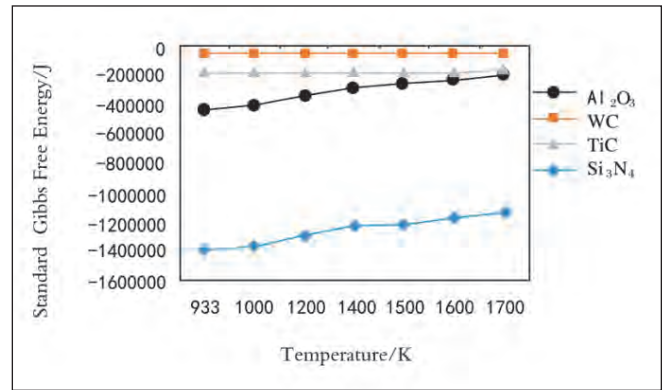


Fig. 26: Comparison of standard gibbs free energy between several compounds

4. Analysis and discussion

(1) From the experiments that Al_2O_3 ceramic tools with workpiece materials including nickel, titanium alloy, 35# steel, cast iron and aluminum alloy, the results show that diffusion amount of element aluminum and oxygen in workpiece is very small, because Al_2O_3 is a compound with much higher stability; compared to other tools materials including tungsten carbide, titanium carbide, silicon nitride and so on, standard free energy of Al_2O_3 is a negative with much greater absolute value, therefore diffusion is hard to happen. From Table 8 and Fig. 26, it is observed that the absolute value of free energy for Al_2O_3 is far higher than that of other three tools material, which shows this compound is much more stable and is hard to be decomposed.

(2) From the comparison of three groups of figures including Figs. 6-8, Figs. 9-11 and Figs. 12-14, the results show that the change amplitude of wave peak when cutting titanium alloy is greatest, and that for pure nickel is greater; the wave peak is most stable when cutting 35# steel. From Figs. 12, 13 and 14, wave peak of line scanning energy wave for aluminum, oxygen and titanium is stable in inspected position when Al_2O_3 ceramic tools cut 35# steel, and the change amplitude of wave peak is also much smaller; this indicates that content change of oxygen element and aluminum element is smaller in wear region of tools and non-cutting region, i.e. dissolution and diffusion concentration of oxygen and aluminum in workpiece material in blades is

TABLE 8. STANDARD FREE GIBBS ENERGY OF SEVERAL COMPOUNDS (K)

Temperature	933	1000	1200	1400	1500	1600	1700
Al_2O_3	-1381317.08	-1359660	-1295012	-1230364	-1198040	-1165716	-1133392
WC	-35948	-35777	-35307	-34852.6	-34626	-34399.4	-34624.5
TiC	-173712	-173027	-170723	-167841	-166398	-164954	-163507.7
Si_3N_4	-428932	-407826	-344824	-281822	-250321	-218820	-192044

very low and tools are hard to make diffusion wear; from the comparison of two groups of figures including Figs. 6-8 and Figs. 9-11, we can know that the change amplitude of wave peak of line scanning energy wave for aluminum, oxygen and titanium in inspected position when Al_2O_3 ceramic tools cut titanium alloy is much greater than that when cutting pure nickel; especially, there is a great decrease for wave value in blades for aluminum and oxygen, content change of oxygen element and aluminum element is smaller in wear region of tools and non-cutting region, i.e. dissolution and diffusion concentration of oxygen and aluminum in workpiece material in blades is very low and tools are hard to make diffusion wear; from the comparison of two groups of figures including Figs. 6-8 and Figs. 9-11, we can know that the change amplitude of wave peak of line scanning energy wave for aluminum, oxygen and titanium in inspected position when Al_2O_3 ceramic tools cut titanium alloy is much greater than that when cutting pure nickel; especially, there is a great decrease for wave value in blades for aluminum and oxygen, which shows that content change of oxygen element and aluminum element is greater in wear region of tools and non-cutting region, i.e. dissolution and diffusion concentration of oxygen and aluminum in workpiece material in blades is much higher than that for cutting pure nickel and tools are easy to make diffusion wear. The reasons include two aspects; one side is that absolute value of excess free energy for these two tool elements in titanium is much greater than that in nickel, so as to be easy to dissolve into titanium; the other side is that the cutting temperature when cutting titanium and aluminum alloy is lower than that for cutting nickel, which indicates that the formation energy is taken out little by cutting metal and absorbed much by tools when cutting. Therefore tools temperature will increase and this strengthens the diffusion degree for tools material in workpiece. From element distributions of cutting elements for three kinds of workpiece materials in Figs. 15-17, aluminum element is not in cutting metal when cutting 35# steel, which shows that aluminum element is hard to diffuse and dissolve into cutting metal, so as hard to be inspected; the content of aluminum and oxygen in tools material when cutting titanium alloy is higher than that for cutting nickel; this also proves that diffusion solubility of tools material in titanium and aluminum alloy is larger than that in pure nickel (Remark: from Fig. 16, we know that content of aluminum when cutting can reach over to 33.62%; the reason is that titanium and aluminum alloy is used as workpiece material; the material contains aluminum in much higher proportion.). The above test conclusions are in accordance with that of the calculation results in this paper.

(3) From Fig. 18 and Figs. 20-22, it indicates that the content of aluminum element in blades increases greatly when Al_2O_3 ceramic tools cut aluminum alloy, which is due to much greater compatibility between Al_2O_3 ceramic tools

and aluminum alloy; therefore it is easy to be clung together when being machined; from the two sets of data in Figs. 12-14 and Figs. 23-25, we can know that there is much greater difference in wear mechanism of tools when machining cast iron and 35# steel under the same cutting condition; though cast iron and 35# steel are both belong to steel material, the workability for 35# steel material is better than that for cast iron in anti-diffusion wear. Because tools wear is a process affected by several nonlinear and strong coupling effects, each kind of effect influences together, which leads to more research on wear mechanism.

5. Conclusions

(1) Solubility of tools material in workpiece material increases with the increase of temperature, which is in exponential function; however, Al_2O_3 a compound with much stronger stability and is hard to be decomposed, the diffusion solubility of Al_2O_3 ceramic tools when machining the above workpiece material is much smaller generally;

(2) Solubility sequence of Al_2O_3 ceramic tools when machining several common workpiece material is as follows: titanium > nickel > steel; at the same cutting temperature, solubility of Al_2O_3 ceramic tools in titanium alloy is greatest, therefore it is not appropriate for machining titanium alloy, on the contrary that in steel material is smallest, so as to be most appropriate for machining steel materials;

(3) At the same cutting condition, when machining cast iron and 35# steel, the wear performance of tools is very different and the wear mechanism should be researched more.

Acknowledgements

The authors gratefully acknowledge the National Natural Science Foundation (No.51465009 and No.61461008); Natural Science Foundation of Guizhou Province (Guizhou Science and Technology Agency J [2014] 2085, J [2014] 2086, LH [2015] 7087); Academician workstation of Guizhou Institute of Technology (Academician workstation (2014) 4007); Department of Education of Guizhou Province 125 project; The doctoral starting up foundation of Guizhou Institute of Technology (XJGC20131201); The First-class University Project of Guizhou Province in 2017 (First-Class Teaching Management Team); The Collaborative education project of Ministry of Education in 2018 (Research on Sharing Alliance system for School-Enterprise courses based on intelligent manufacturing and building of practice base on innovation education).

References

1. Ramirez C, Idhil Ismail A, Gendarme C, Dehmas M, Aeby-Gautier, E., Poulachon G, Rossi F.(2017): "Understanding the diffusion wear mechanisms of WC-10%Co carbide tools during dry machining of titanium alloys". *Wear*, 390-391,61-70.

2. Fábio F. Lima, Wisley F. Sales, Eder S. Costa, Flávio J. da Silva, Álisson R. Machado. (2017): "Wear of ceramic tools when machining Inconel 751 using argon and oxygen as lubricating atmospheres". *Ceramics International*, 43(1), 677-685.
3. Oliver Hatt, Pete Crawforth, Martin Jackson. (2017): "On the mechanism of tool crater wear during titanium alloy machining". *Wear*, Volumes 374–375, 15 March 2017,15-20.
4. Elyas, Hawsawi, Kim Tae Woo, Jang Byung-Koog, Lee Kee Sung. (2018): "Damage and wear resistance of Al_2O_3/SiC microcomposites with hard and elastic properties". *Journal of the Ceramic Society of Japan*, 126(1),21-26.
5. Murthy T.S.R.C, Ankata Sairam, Sonber J.K, Sairam K, Singh Kulwant, Nagaraj A, Sengupta P, Bedse R.D, Majumdar Sanjib, Kain Vivekanand Microstructure.(2018): "Thermo-physical, mechanical and wear properties of in-situ formed boron carbide-Zirconium diboride composite". *Ceramics-Silikaty*, 62(1),15-30.
6. Shao Fang, Wang Yuting, Xiao Yingqun, Xiao Lihua, Zhang Kesheng, Cai Qun.(2016): "Wear of PCBN tool when cutting materials difficult-to-cut based on thermodynamics solubility". *Key Engineering Materials*, 693,1207-1215.
7. L.A.Sosnovskiy, S.S.Sherbakov.(2012): "Mechanothermal dynamical system and its behavior", *Continuum Mechanics and Thermodynamics*, 24(3),239-256.
8. S. Phapale, R. Shukla, R. Mishra; A.K. Tyagi.(2014): "Standard molar enthalpy of formation of $Ce_2Zr_2O_8$ ", *Journal of Alloys and Compounds*. 615,792-794.
9. Liu Shuhong; Ling Dicheng, Huang Dandan, Zhang Fan, Du Yong.(2015): "Multi-element aluminum alloy phase diagram thermodynamics, thermophysical properties database and its application". *Progress in Chinese Materials*, 34(4), 305-316.
10. C.L. Pu, G. Zhu, S.B. Yang, E.B. Yue, S.V. Subramanian. (2016): "Effect of dynamic recrystallization at tool-chip interface on accelerating tool wear during high-speed cutting of AISI1045 steel". *International Journal of Machine Tools and Manufacture*. 1 (100),72–80.
11. Guo Cheng Wang, Qi Wang, Sheng Li Li, Xin Gang Ai, Da Peng Li.(2015): "A Multi-step Thermodynamic Model for Alumina Formation during Aluminum Deoxidation in Fe–O–Al Melt", *Acta Metallurgica Sinica (English Letters)*. 28(2), 272-280.
12. Wang Dan, Zhou Xiaoping. (2016): "Thermodynamic analysis of $Al_2O_3-AlB_{12}$ ceramic powder prepared by mechanical alloying". *Chinese Journal of Rare Metals*, 40(4), 334-338.

AN EXPERIMENTAL STUDY OF CRACK PROPAGATION REGULARITY MONITORED
IN FRACTURE GROUTING IN CLAY

Continued from page 653

References

1. Alfaro, M.C., Wong, R.C. (2001): "Laboratory studies on fracturing of low-permeability soils". *Canadian Geotechnical Journal*, 38(2), 303-315.
2. Kleinlugtenbelt, R., Bezuijen, A., et al.(2006): "Model tests on compensation grouting". *Tunnelling and Underground Space Technology*, 21(3-4), 435-436.
3. Bezuijen, A., et al. (2007): "Laboratory tests on compensation grouting, the influence of grout bleeding". Proc., 33rd ITA-AITES World Tunnel Congress. New York: Taylor and Francis, 395-401.
4. Bezuijen, A., van Tol F. (2007): "Compensation grouting in sand, fractures and compaction", Pro. Conf. on Soil Mechanics and Geotechnical Engineering, 1257-1262.
5. Zhang Z M, Zou J, He J Y, et al.(2009):"Laboratory tests on compaction grouting and fracture grouting of clay". *Chinese Journal of Geotechnical Engineering*, 31(12):1818-1824.
6. Zhang Q S, Zhang L Z, Liu R T, et al. (2016): "Split grouting theory based on slurry-soil coupling effects". *Chinese Journal of Geotechnical Engineering*, 38(2), 323-330.
7. SUN, F., CHEN, T., et al. (2009): "Study on Fracture Grouting Mechanism in Subsea Tunnel Based on Bingham Fluids". *Journal of Beijing Jiaotong University*, 33(4), 1-6.
8. Zhang Z M, Zou J.(2008):"Penetration radius and grouting pressure in fracture grouting". *Chinese Journal of Geotechnical Engineering*, 30(2), 181-184.
9. Bezuijen, A., et al. (2011): "Analytical Model for Fracture Grouting in Sand". *Journal of Geotechnical and Geoenvironmental Engineering*, 137(6), 611-620.
10. Chen, T. L., Zhang, L. Y., and Zhang, D. L.(2014): "An FEM/VOF hybrid formulation for fracture grouting modelling". *Computers and Geotechnics*, 58(58),14-27.
11. Sarris, E., Papanastasiou, P. (2013): "Numerical modeling of fluid-driven fractures in cohesive poroelastoplastic continuum". *International Journal for Numerical and Analytical Methods in Geomechanics*, 37(12), 1822-1846.
12. Lecampion B. (2009): "An extended finite element method for hydraulic fracture problems ". *Communications in Numerical Methods in Engineering*, 25(2), 121–133.
13. Frangi A., Novati G., et al.(2002): "3D fracture analysis by the symmetric Galerkin BEM ". *Computational Mechanics*, 28(3-4), 220-232.
14. Min, K. B., Jing, L. (2003): "Numerical determination of the equivalent elastic compliance tensor for fractured rock masses using the distinct element method". *International Journal of Rock Mechanics and Mining Sciences*, 40(6), 795-816.
15. Tan, X. C., Kou, S. Q., and Lindqvist, P. A. (1998): "Application of the DDM and fracture mechanics model on the simulation of rock breakage by mechanical tools", *Engineering Geology*, 49(3-4), 277-284.